JOURNAL OF NATURAL PRODUCTS

Subscriber access provided by ISTANBUL TEKNIK UNIV

Isolation and Structure of Cephalostatins 10 and 11

George R. Pettit, Jun-Ping Xu, Michael D. Williams, Nigel D. Christie, Dennis L. Doubek, Jean M. Schmidt, and Michael R. Boyd

J. Nat. Prod., **1994**, 57 (1), 52-63• DOI:
10.1021/np50103a007 • Publication Date (Web): 01 July 2004

Downloaded from http://pubs.acs.org on April 4, 2009

More About This Article

The permalink http://dx.doi.org/10.1021/np50103a007 provides access to:

- Links to articles and content related to this article
- Copyright permission to reproduce figures and/or text from this article

ACS Publications
High quality. High impact.

Journal of Natural Products is published by the American Chemical Society. 1155 Sixteenth Street N.W., Washington, DC 20036

Journal of Natural Products
Vol. 57, No. 1, pp. 52-63, January 1994

ISOLATION AND STRUCTURE OF CEPHALOSTATINS 10 AND 11[1]

GEORGE R. PETTIT,* JUN-PING XU, MICHAEL D. WILLIAMS, NIGEL D. CHRISTIE, DENNIS L. DOUBEK, JEAN M. SCHMIDT,

Cancer Research Institute and Department of Chemistry, Arizona State University, Tempe, Arizona 85287-1604

and MICHAEL R. BOYD

Laboratory of Drug Discovery Research and Development, DTP, DCT, National Cancer Institute, FCRDC, Frederick, Maryland, 21702-1201

ABSTRACT.—Further investigation of antineoplastic constituents from the marine worm *Cephalodiscus gilchristi*, employing a 450 kg re-collection from the Indian Ocean (Southeast Africa), has led to isolation and structural determination of two previously undetected members of the cephalostatin series, designated cephalostatins 10 [**4**] and 11 [**5**]. Structural analyses were conducted primarily employing high field 2D nmr and high resolution mass spectral techniques. All the stereochemical assignments were deduced using the original X-ray crystal structure of cephalostatin 1 and ROESY 2D nmr methods. Both cephalostatins 10 and 11 strongly inhibited growth of a series of important human cancer cell lines.

Marine organisms continue to be a rich source of many unusual steroids, and a considerable number have been investigated chemically and pharmacologically (2–11). As part of our extensive twenty-year investigation of antineoplastic constituents in the tube-inhabiting marine worm *Cephalodiscus gilchristi* (12), a member of the class Pterobranchia (phylum Chordata, Hemichordata subphylum), the remarkable disteroidal alkaloids, cephalostatins 1–9, were discovered (12–15). They were found to have exceptionally potent activity against a series of human cancer cell lines and the murine P-388 lymphocytic leukemia cell line (PS system) (15). Among them cephalostatins 1 [**1**] and 7 [**3**] proved to be the most powerful cell growth inhibitors against P-388 (ED_{50} 10^{-7}–10^{-9} μg/ml). Further PS cell line activity-guided investigation of *C. gilchristi* employing a 1990 scale-up re-collection (450 kg, wet wt) has led to the discovery of two new disteroidal alkaloids, herein named cephalostatins 10 [**4**] and 11 [**5**]. Both display considerable in vitro cytotoxicity against a very important series of human cancer cell lines. A description of the isolations and complete structure determinations of these new cephalostatins follows.

C. gilchristi was again collected by scuba (ca. −20 m) in the Indian Ocean off Southeast Africa. After extraction and preliminary solvent partition separations, the PS-active (ED_{50} 2.5×10^{-1} μg/ml) CH_2Cl_2 fraction was successively partitioned (16) between MeOH-H_2O (9:1) and hexane, then diluted to MeOH-H_2O (3:2) and extracted with CH_2Cl_2 (16). The resulting CH_2Cl_2 fraction significantly inhibited (ED_{50} 4.4×10^{-2} μg/ml) the P-388 leukemia. Initial gel-permeation chromatographic separations of this fraction on Sephadex LH-20 in MeOH and again with CH_2Cl_2-MeOH (3:2) as eluents led to a further concentration of activity. Further separations were achieved employing successive partition chromatographies on Sephadex LH-20 [hexane-toluene-MeOH (3:1:1), hexane-iPrOH-MeOH (8:1:1), and hexane-CH_2Cl_2-MeOH (5:1:1)] to give several fractions rich in the active components. Final purification by reversed-phase hplc (C-8) using MeCN-MeOH-H_2O (10:10:12) as eluent afforded cephalostatins 10 [**4**] (14.6 mg, 3.24×10^{-6}% yield) and 11 [**5**] (6.1 mg, 1.36×10^{-6}% yield).

[1]Antineoplastic Agents series number 271. For part 270, see Berkow *et al.* (1).

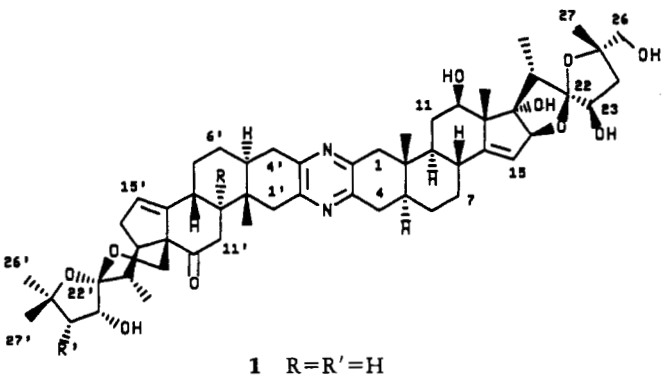

1 R=R′=H
2 R=OH, R′=H

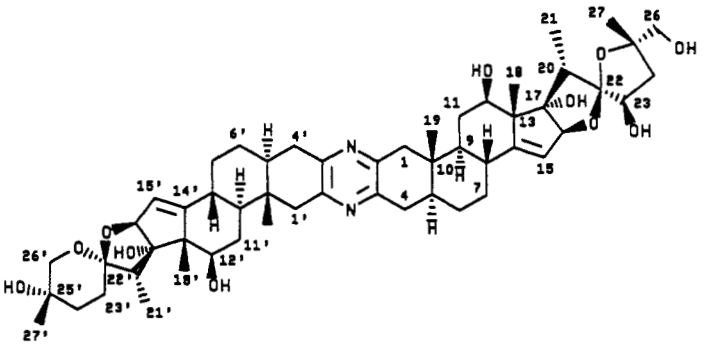

3

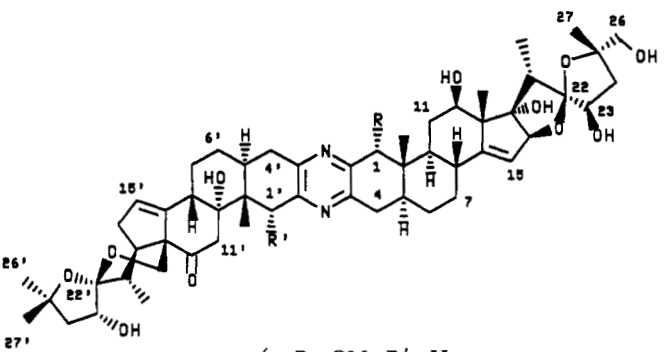

4 R=OMe, R′=H
5 R=H, R′=OMe

Cephalostatins 10 [**4**] and 11 [**5**] were obtained as colorless amorphous powders. Both were optically active and exhibited uv absorptions at 289 (log ε 4.08) and 304 (shoulder) nm, which suggested the presence of a pyrazine ring system typical of the cephalostatins. Hrfabms results indicated that pyrazines **4** and **5** both corresponded to molecular formula $C_{55}H_{77}N_2O_{12}$ with $[M+H]^+$ at 957.5492 and 957.5474, respectively (calcd 957.5491). The ^{1}H-nmr, ^{13}C-nmr (Tables 1 and 3) and fabms spectra of cephalostatins 10 and 11 suggested structures similar to cephalostatin 2 [**2**] with an additional OMe. Interpretation of the cephalostatin 10 nmr showed that signals earlier (13) attributed to the "left-side" steroid unit in cephalostatin 2 all appeared to be normal. However, for the first time, the "right-side" steroid unit was found to differ from that of all other cephalostatins.

TABLE 1. The High Field (500 MHz) ^{1}H- and ^{13}C-nmr Spectral Data in Cephalostatin 10 [4] and Assignments (in C,D,N).

Position	Right side				Position	Left side			
	^{13}C ppm	^{1}H ppm	*J* (Hz)	HMBC (H to C)		^{13}C ppm	^{1}H ppm	*J* (Hz)	HMBC (H to C)
1	83.38 d	4.15 s		2,3,5,19, 10, OMe	1′	39.75 t	2.99 m		2′,5′,9′,10′,19′
							3.74 m		2′,5′,9′,10′,19′
OMe	57.31 s								
2	149.90 s				2′	150.01 s			
3	147.54 s				3′	147.67 s			
4	35.77 t	3.00 m			4′	36.19 t	2.73 m		3′,5′,10′
		2.61 m					3.06 dd	17.0,6.0	3′,5′,10′
5	35.14 d	2.27 m			5′	34.23 d	2.55 m		
6	28.33 t	1.28 m			6′	28.12 t	1.48 m		
		1.52 m						1.70 m	
7	28.61 t	1.34 m			7′	24.56 t	1.90 m		
		1.64 m						2.02 m	
8	33.68 d	2.13 m			8′	39.00 d	2.75 m		
9	45.91 d	0.85 m			9′	78.64 s			
10	40.67 s				10′	41.25 s			
11	28.76 t	1.85 m		9	11′	45.58 t	2.96 m		8′,9′,10′,13′
		2.12 m		9			3.31 m		8′,9′,10′,13′
12	75.70 d	4.24 m			12′	210.99 s			
13	55.46 s				13′	61.55 s			
14	153.08 s				14′	148.46 s			
15	122.20 d	5.62 brs		8,13,14, 16,17	15′	123.76 d	5.56 brs		8′,13′,14′, 16′,17′
16	93.23 d	5.24 brs		15,17,22	16′	32.55 t	2.27 m		13′
							2.92 m		13′
17	91.72 s				17′	44.19 d	2.80 m		13′,16′,22′

TABLE 1. Continued.

Position	Right side				Position	Left side			
	^{13}C ppm	^{1}H ppm	*J* (Hz)	HMBC (H to C)		^{13}C ppm	^{1}H ppm	*J* (Hz)	HMBC (H to C)
18	12.65 q	1.34 s		12,13,14,17	18′	64.03 t	4.14 dd	12.0	13′,17′
19	11.06 q	0.71 s		1,5,9,10	19′	15.06 q	0.98 s		1′,5′,9′,10′
20	44.52 d	2.87 m		13,17,23	20′	32.87 d	3.18 m	13.2,6.0	16′,17′,21′,22′
21	9.02 q	1.35 d	7.0	17,20,22	21′	15.47 q	1.39 d	6.6	17′,20′,22′
22	117.15 s				22′	110.94 s			
23	71.56 d	4.81 m			23′	81.59 d	4.83 m		22′,25′
24	39.45 t	2.35 m		23,25,26,27	24′	47.34 t	1.94 m		23′,26′,27′
		2.70 m		23,25,26,27			2.35 m		23′,26′,27′
25	82.79 s				25′	81.13 s			
26	69.29 t	3.80 d	11.0	25,27	26′	29.79 q	1.47 s		24′,25′,27′
		3.72 d	11.0	25,27					
27	26.40 q	1.63 s		24,25,26	27′	29.52 q	1.40 s		24′,25′,26′
17-OH		6.23 s		13,17	9′-OH		5.97 s		8′,9′,10′,11′
12-OH		4.79 s		12					

TABLE 2. Cephalostatin 10 [**4**] NOe Effects from ROESY (500 MHz, in C_5D_5N).

Proton	Left side		Proton	Right side	
	δ	nOe		δ	nOe
H-1α	3.74	H-5α, 9-OH	1-OMe ..	3.50	H-9α, H-11α, H-1β
H-1β	2.99	Me-19	H-1β....	4.15	Me-19, H-11α, 1α-OMe
H-4α	3.06	H-5α, H-6α	H-4α....	3.00	H-5α
H-4β	2.73	H-6β	H-4β....	2.61	H-6β, Me-19
H-5α	2.55	H-1α, H-4α, H-6α	H-5α....	2.27	H-4α, H-6α, H-9α
H-6α	1.70	H-4α, H-5α, H-7β	H-6α....	1.52	H-4α, H-5α, H-7α
H-6β	1.48	H-4β, H-8β, Me-19	H-6β....	1.28	H-4β, H-7β, Me-19
H-7α	2.02	H-15	H-7α....	1.34	H-5α, H-9α, H-15
H-7β	1.90	H-15	H-7β....	1.64	H-15
H-8β	2.75	H-6β, H-11β, H-18, Me-19	H-8β....	2.13	H-6β, H-7β, H-11β, Me-18, Me-19
9-OH.....	5.97	H-1α, H-11α, H-5α	H-9α....	1.86	H-11α, H-12α, H-5α
H-11α	2.96		H-11α...	2.12	H-12α, H-9α, H-1β
H-11β	3.31	H-8β, H-18, Me-19	H-11β...	1.85	H-8β, Me-18, Me-19
			H-12α...	4.24	H-9α, H-11α
H-15	5.57	H-7α, H-7β, H-16β H-16α	H-15	5.62	H-7α, H-7β
H-16α	2.27	H-21	H-16α...	5.24	H-15, 17-OH
H-16β	2.92	H-15, Me-21			
H-17α	2.80	H-16α, Me-21	17-OH ..	6.23	H-23α, H-12α, H-16, Me-21
H-18	4.14	H-11β, H-8β, Me-27	Me-18 ...	1.34	H-8β, H-11β, H-20β
Me-19	0.98	H-1β, H-6β, H-8β, H-11β	Me-19 ...	0.71	H-1β, H-4β, H-6β, H-8β, H-11β
H-20β	3.18	H-17α, H-21	H-20β...	2.87	Me-18
Me-21	1.39	H-17α, H-16α, H-16β	Me-21 ...	1.35	H-23α, 17-OH
H-23β	4.83	H-24β	H-23α...	4.81	Me-21, H-24α, 17-OH
H-24α	1.94	Me-26	H-24α...	2.70	H-23α
H-24β	2.35	H-23α, Me-27	H-24β...	2.35	Me-27
Me-26	1.47	H-24α	H-26....	3.76	H-24α, Me-27
Me-27	1.40	H-24β, H-18	Me-27 ...	1.63	H-26, H-24β

The cephalostatin 10 [**4**] H,H-COSY, TOCSY, and XHCOSY 2D nmr experiments indicated that four spin systems, $-CH_2-CH-CH_2-CH_2-CH-CH-CH_2-$, $=CH-CH-O-$, $HO-CH-CH_2-$, and CH_3-CH-, were present in the "right-side" steroid unit, analogous to cephalostatins 1–9. But one signal (^1H 4.15 ppm, s) related to a carbon (^{13}C 83.38 ppm, d) showed that all the carbons adjacent to this carbon were quaternary and the spectral relationships due to C-9 (^1H 0.80 ppm, m related to ^{13}C 53.00 ppm, d) of cephalostatins 1–9 had disappeared. Hmbc cross peaks were observed between the single proton at C-1 and C-10 (δ 40.66, s), C-5 (δ 35.14, d), C-2 (δ 149.90, s), C-3 (δ 147.55, s), C-19 (δ 11.06, q), as well as with the OMe (δ 57.31, q). Therefore, this signal was assigned as H-1 and the methoxy group was located at the C-1 position of the "right-side" steroid unit.

As recorded in Table 2, the 2D rotating Overhauser spectrum (ROESY) (17) of cephalostatin 10 [**4**] showed nOe's between H-1 (δ 4.15) and the Me-19, H-11α and the 1-OMe as well as between the 1-OMe and H-9α, and between the H-11α and H-1. Such data indicated the H-1 must be above the face of the ring whereas the 1-OMe must be in a pseudoaxial position below the face of the ring (Figure 1). Based on our earlier X-ray crystal structure determination of cephalostatin 1, this evidence completed the stereochemical assignments for cephalostatin 10.

All the cephalostatin 11 [**5**] nmr signals were analyzed using APT, ^1H, ^1H-COSY,

TABLE 3. Cephalostatin 11 [**5**] ^{1}H- and ^{13}C-nmr Spectral Data and Assignments (500 MHz, in C$_5$D$_5$N).

Position	Right side				Position	Left side			
	^{13}C ppm	^{1}H ppm	*J* (Hz)	HMBC (H to C)		^{13}C ppm	^{1}H ppm	*J* (Hz)	HMBC (H to C)
1	46.12 t	2.60 m		2,5,10	1′	85.84 d	4.58 m		2′,5′,10′,OMe
		3.10 d	17.0	2,5,10	OMe	56.59 q	3.35 s		1′
2	151.97 s				2′	149.37 s			
3	148.35 s				3′	145.90 s			
4	35.69 t	2.95 m		2,3,19	4′	35.78 t	2.65 m		3′,5′,10′
		2.62 m		2,3,19			3.20 dd	18.0,6.0	3′,5′,10′
5	41.70 d	1.59 m			5′	28.89 d	2.00 m		
6	28.17 t				6′	29.98 t	1.39 m		
7	28.17 t				7′	24.38 t	1.85 m		
							2.07 m		
8	33.75 d	2.07 m			8′	39.47 s	2.65 m		
9	53.11 d	0.86 m			9′	80.24 s			
10	36.33 s				10′	43.10 s			
11	28.64 t	1.77 m			11′	46.56 t	2.87 m		8′,9′,12′
		2.05 m					3.42 d	13.5	8′,9′,12′
12	75.52 d	4.05 dd	11.0,4.2		12′	210.74 s			
13	55.37 s				13′	61.59 s			
14	152.63 s				14′	148.03 s			
15	122.30 d	5.64 brs		8,13,14,17	15′	123.76 d	5.56 brs		13′,16′,17′
16	93.14 d	5.24 brs		22	16′	32.47 t	2.31 m		
							2.85 m		
17	91.62 s				17′	44.23 d	2.90 m		
18	12.61 q	1.33 s		12,13,14,17	18′	64.59 t	4.15 dd	11.0	12′,17′
19	11.76 q	0.76 s		1,5,9,10	19′	14.40 q	0.81 s		1′,5′,9′,10′
20	44.49 d	2.82 m		17,23	20′	32.95 d	3.25 m		16′,17′,21′,22′
21	8.97 q	1.35 d	7.2	17,20,22	21′	15.89 q	1.43 d	6.7	20′,22′
22	117.15 s				22′	110.94 s			
23	71.50 d	4.81 m			23′	81.60 d	4.81 m		
24	39.47 t	2.36 m		23,25,26,27	24′	47.29 t	1.93 dd	12.0,6.0	22′,23′,25′,26′
		2.75 m		23,25,26,27			2.35 m		
25	82.82 s				25′	81.11 s			
26	69.25 t	3.80 d	13.5	25,27	26′	29.74 q	1.47 s		25′,27′
		3.72 d	13.5	25,27					
27	26.41 q	1.64 s		24,25,26	27′	29.48 q	1.40 s		24′,25′,26′
17-OH		6.23 s		15,16	9-OH		5.95 s		8′,10′,11′

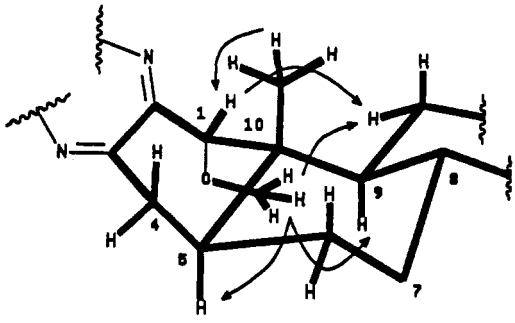

FIGURE 1. Partial nOe correlations in the right side A/B ring unit of cephalostatin 10 [**4**].

TOCSY, HMQC, and HMBC techniques and clearly indicated that nmr signals due to the "right-side" steroid unit in cephalostatin 11 [**5**] were the same as those found in cephalostatins 1–9. In addition, three spin systems, $-CH_2-CH-CH_2-CH_2-CH-$, $=CH-CH_2-CH-CH-CH_3$, $HO-CH-CH_2$, that were identified in the "left-side" steroid unit of cephalostatin 11 [**5**] were the same as shown by cephalostatin 10 [**4**]. Since the proton attached to C-1′ (δ 85.84, d) gave a singlet signal (δ 4.58), the methoxyl group was placed at C-1′ following the series of deductions already summarized above for cephalostatin 10. Meanwhile, this result was confirmed by the long-range coupling interactions seen in the HMBC spectrum, (cf. Figure 2) between H-1′ and 1′-OMe, H-1′ and C-10′, and Me-19′ and C-1′ (Table 3). Furthermore, the ^{13}C chemical shift of C-9′ was observed downfield approximately 1.5 ppm compared to that of cephalostatin 10 [**4**]. From this evidence it was assumed that the methoxyl group at C-1′ had the α configuration, and this was further suggested by hydrogen bonding between the methoxyl at C-1′ and the hydroxyl at C-9′ (see Figure 3). ROESY interactions between H-1′β and Me-19′ as well as between 1′α-OMe and H-5′α, H-11′α and 9′α-OH confirmed this stereochemical assignment (Figure 3).

The remaining nOe correlations arising from cephalostatins 10 and 11 were similar. The nOe effect between H-12 and H-9α in the "right-side" unit established the 12-OH β configuration. NOe's detected between H-23 and the Me-21 as well as 17α-OH in the "right-side" unit suggested that the 23-OH should have the β configuration. Also, in the "left-side" unit the Me-21′ showed ROESY correlations to H-17α, H-16α, and H-

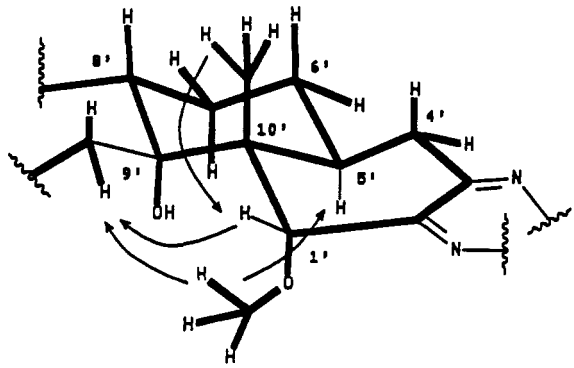

FIGURE 2. Selected A/B ring nOe correlations in the left side unit of cephalostatin 11 [**5**].

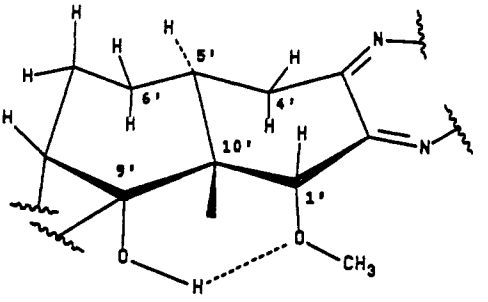

FIGURE 3. Hydrogen bonding between the C-1′ methoxyl and the C-9′ hydroxyl in cephalostatin 11 [**5**].

16β. Other nOe experiments (Tables 2 and 4) confirmed the stereochemical relationships (Figures 4 and 5) of cephalostatins 10 and 11 to cephalostatins 1 and 2.

In the U.S. National Cancer Institute's (NCI) new in vitro, human cancer focused evaluation system (18–21), cephalostatins 10 [**4**] and 11 [**5**] proved to be very potent and selective. Comparative antitumor evaluations of cephalostatins 1 [**1**], 10 [**4**], and 11 [**5**] in the NCI's disease-oriented, in vitro primary screen (19) revealed an overall potency of **4** and **5** approaching that of **1** and mean graph profiles (18,20) of **4** and **5**

TABLE 4. NOe Effects Displayed by Cephalostatin 11 [**5**] from ROESY (500 MHz, in C_5D_5N).

Proton	Left side		Proton	Right side	
	δ	nOe		δ	nOe
1-OMe	3.35	H-1β, H-11α, 9-OH	H-1α....	2.60	H-5α, H-9α
H-1β	4.58	1-OMe, H-11α, 19-Me	H-1β....	3.10	Me-19, H-11α
H-4α	3.20		H-4α....	2.95	H-5α
H-4β	2.65	Me-19	H-4β....	2.62	Me-19, H-6β
H-5α	2.00		H-5α....	1.59	H-4α, H-9α
H-7α	2.07	H-15	H-7α....	1.32	H-15
H-7β	1.85	H-15	H-7β....	1.70	H-15
H-8β	2.65	H-18	H-8β....	2.07	Me-19, Me-18, H-11β
9-OH.....	5.70	1-OMe, H-11α	H-9α....	0.87	H-1α, H-12α
H-11α	2.87	H-1β	H-11α...	2.05	H-1β
H-11β	3.42	H-18, Me-19, H-8β	H-11β...	1.77	Me-19, Me-18
			H-12α...	4.05	12-OH, H-11α, H-9α
			12-OH	4.70	Me-18, H-12α
H-15	5.56	H-7β, H-16β, H-7α, H-16α	H-15....	5.64	H-7β, H-16β, H-7α
H-16α	2.31	H-17α	H-16α...	5.24	H-15, 17-OH
H-16β	2.85				
H-17	2.90	Me-21, H-20, H-16α	17-OH ..	6.23	Me-21, H-16α
H-18	4.15	H-8β, H-11β	Me-18 ...	1.33	H-8β, H-11β
Me-19	0.81	H-1β, H-8β, H-11β, H-4β	Me-19 ...	0.76	H-1β, H-4β, H-8β, H-11β
H-20	3.25	Me-21, H-17α	H-20....	2.82	Me-21, Me-18
Me-21	1.43	H-16α, H-17α, H-20	Me-21 ...	1.35	H-23α, H-20
H-23β	4.82	H-24β	H-23α...	4.81	Me-21, H-24α
H-24α	1.93	Me-26	H-24α...	2.75	H-23α
H-24β	2.35	Me-27, H-23β	H-24β...	2.36	Me-27
Me-26	1.47	H-24α	H-26....	3.76	Me-27, H-24α
Me-27	1.40	H-18, H-24β	Me-27 ...	1.64	H-26, H-24β

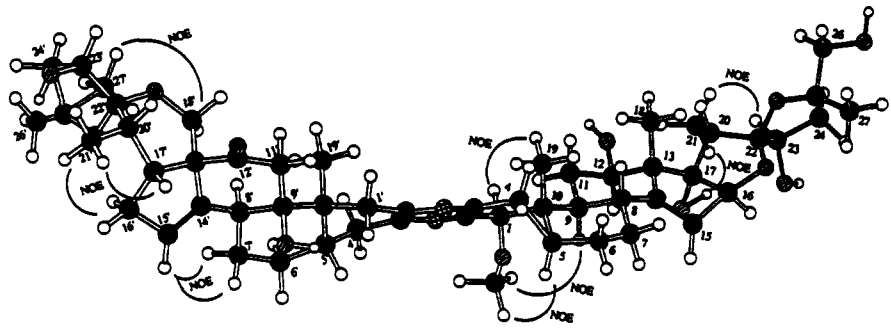

FIGURE 4. The stereochemical structure of cephalostatin 10 [**4**] and principal nOe correlations.

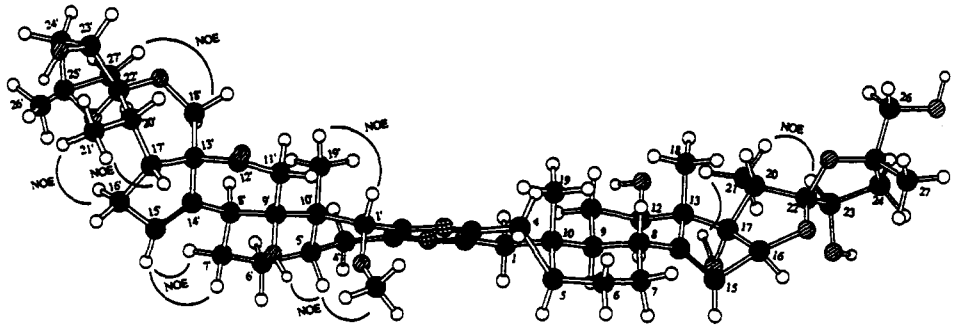

FIGURE 5. The stereochemical structure of cephalostatin 11 [**5**] and strong nOe correlations.

which were highly correlated with that of **1** (Table 5). The distinctive mean graph "fingerprint" shared by the cephalostatins is shown in Figure 6. Individual cell line identifiers are provided in the Experimental section. The cephalostatins demonstrate one of the most extreme examples of differential cytotoxicity yet encountered in the NCI screen (M.R. Boyd, unpublished observations); as illustrated herein, the variation in sensitivity among the different lines spans as much as 1000- to 10,000-fold. For example, adriamycin (22) typically ranges from negative $\log_{10}$ GI_{50} values of 5.9 to 8.4 while cephalostatin 1 displays GI_{50} values of 7.2 to 10.6. As such, the cephalostatins provide an important prototype lead from the new NCI in vitro primary screen for

TABLE 5. Results of Comparative Antitumor Evaluations of Cephalostatins 1 [**1**], 10 [**4**], and 11 [**5**] in the NCI In Vitro Primary Screen.[a]

Compound	Mean Panel GI_{50} ($\times 10^{-9}$ M)[b]	Compare Correlation Coefficient[c]
1	1.2	1.00
4	4.1	0.88
5	11.0	0.89

[a]All compounds were tested in quadruplicate at each of three different concentration ranges (10^{-6},10^{-7}, and 10^{-8} M upper limits; $\log_{10}$ dilutions×5) against the entire panel of 60 human tumor cell lines comprising the NCI screen.

[b]Standard errors averaged less than 15% of the respective means.

[c]Correlation coefficients from the Compare pattern-recognition algorithm were calculated by computer using the TGI-centered mean graph profiles of differential cellular sensitivities to **1**, **4**, and **5**. The TGI mean graph profile of **1** was used as the "seed" for the comparisons.

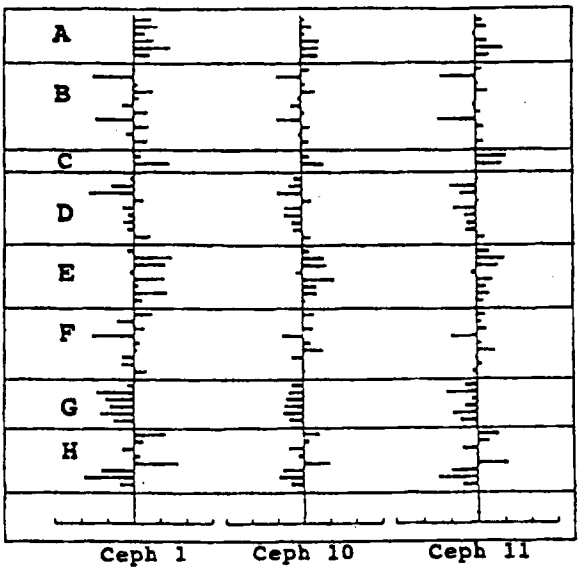

FIGURE 6. Averaged, GI_{50}-centered mean graphs from quadruplicate testing of compounds **1**, **4**, and **5** in the NCI in vitro primary screen (18–20). The tumor cell line subpanels are identified as follows: A (leukemia), B (non small-cell lung), C (small-cell lung), D (colon), E (brain), F (melanoma), G (ovary), H (kidney). Bars projecting to the right of the central reference lines represent the more sensitive cell lines; bars to the left represent less sensitive cell lines. Individual cell line identifiers are provided in the Experimental section. The scaling marks at the bottom of each mean graph represent ± 3 $\log_{10}$M concentration units.

detailed in vivo pharmacologic and xenograft evaluation against selected sensitive human tumor lines.

EXPERIMENTAL

GENERAL PROCEDURES.—Solvents were freshly distilled. Sephadex LH-20, particle size 25–100 μm used in gel permeation and partition column chromatographic separations was obtained from Pharmacia Fine Chemicals AB, Uppsala, Sweden. The tlc plates were viewed under shortwave uv light and then developed by 20% H_2SO_4 or 3% $Ce(SO_4)_2$/3 N H_2SO_4 spray reagent followed by heating at approximately 150°. For hplc separations, a Phenomenex Prepex (particle size 5–20 μ, ϕ 10.0 mm×25 cm) C-8 column was used in reversed-phase mode with Altex (Model 110A) solvent metering pumps and Gilson Holochrome HM uv detection at 288 nm.

Uncorrected melting points were observed with a Kofler-type mp apparatus. Optical rotations were determined employing a Perkin-Elmer Model 241 polarimeter. The uv spectra were obtained using a Hewlett-Packard 8450 uv-vis spectrometer. The ^{1}H-nmr, ^{13}C-nmr, and APT spectra were recorded in C_5D_5N using TMS as an internal standard with a Bruker AM-400 instrument and ASPECT-3000 computer. The ^{1}H,^{1}H-COSY, ^{13}C,^{1}H-COSY, TOCSY (mixing time of 45 msec and 60 msec), HMQC (optimized for $^1J_{H\text{-}C}=140$ Hz), HMBC (optimized for $^nJ_{H\text{-}C}=8.2$ Hz), and ROESY (mixing time of 100 msec and 150 msec) data were obtained using a Varian 500 nmr spectrometer. Hrfabms were obtained employing a Kratos MS-50 spectrometer.

ANIMAL EXTRACTION AND SOLVENT PARTITION SEQUENCE.—*C. gilchristi* (12) was re-collected as the intact worm tube (coenecium) in June–August 1990 in the Indian Ocean off Southeast Africa by scuba (ca. −20 m). A voucher specimen is maintained in the Arizona State University, Cancer Research Institute. The marine worm (450 kg, wet wt) was extracted with 70% MeOH for 4 months, followed by two more extractions with MeOH/CH_2Cl_2 and the CH_2Cl_2 phase separated by adding H_2O. The MeOH extract was

concentrated and partitioned three times between CH_2Cl_2 and H_2O. The combined CH_2Cl_2 extract (1.21 kg) was successively partitioned using the system MeOH-H_2O (9:1→3:2) against hexane→CH_2Cl_2, respectively, to yield the active CH_2Cl_2 fraction (97 g, PS ED_{50} 4.4×10^{-2} μg/ml).

ISOLATION OF CEPHALOSTATINS 10 [**4**] AND 11 [**5**].—Bioassay-guided separation of the active CH_2Cl_2 fraction proceeded as follows. Six fractions (A–F) were obtained from the active CH_2Cl_2 fraction by Sephadex LH-20 chromatography using MeOH as eluent. Active fraction C (29.7 g; PS ED_{50} 2.1×10^{-3} μg/ml) was chromatographed on LH-20 in CH_2Cl_2-MeOH (3:2) to give two main fractions (G and H). The PS cell line most active fraction H (PS ED_{50} 3.5×10^{-4} μg/ml) was further separated on an LH-20 column with hexane-toluene-MeOH (3:1:1) elution to provide nine fractions (I–Q). The most active fraction M (PS ED_{50} 5.3×10^{-4} μg/ml) was subjected to successive partition column chromatographic steps using LH-20 with hexane-iPrOH-MeOH (8:1:1) and hexane-CH_2Cl_2-MeOH (5:1:1) as eluents. Final separation and purification were achieved by C-8 reversed-phase hplc techniques with MeOH-MeCN-H_2O (10:10:13) as mobile phase. By this means two pure and PS cytostatic substances were isolated. Cephalostatin 10 [**4**] (14.6 mg, 3.24×10^{-6}% yield, PS ED_{50} 3.0×10^{-3} μg/ml): mp >300°, $[\alpha]_D$ +80° (c=0.17, MeOH); uv (MeOH) λ 289 (log ε 4.08), 304 (shoulder) nm; hrfabms m/z $[M+H]^+$ 957.5492 ($C_{55}H_{77}N_2O_{12}$ calcd 957.5444). Cephalostatin 11 [**5**] (6.1 mg, 1.36×10^{-6}% yield, PS ED_{50} 2.5×10^{-3} μg/ml): mp >300°, $[\alpha]_D$ +75° (c=0.13, MeOH); uv (MeOH) λ 288 (log ε 3.96), 305 (shoulder) nm; hrfabms m/z $[M+H]^+$ 957.5474 ($C_{55}H_{77}N_2O_{12}$ calcd 957.5444). The ^1H, ^{13}C nmr, ^1H-^{13}C long-range correlations from HMBC and nOe assignments have been recorded in Tables 1–4.

BIOLOGICAL EVALUATION.—The rationale and the technical details of how the NCI in vitro primary screening assay is performed and how the data calculations are applied are described elsewhere (18–20). Figure 6 is a composite of averaged GI_{50} mean graphs prepared for compounds **1**, **4**, and **5**, each tested in quadruplicate. The individual cell line names, in the order as arranged from top to bottom in the mean graphs, are provided as follows, along with the respective negative $\log_{10}$ GI_{50} values for the benchmark compound **1**: CCRF-CEM (9.60), HL-60 TB (9.82), K-562 (9.37), MOLT-4 (9.70), RPMI-8226 (10.29), SR (9.54), A549/ATCC (8.96), EKVX (7.36), HOP-18 (9.08), HOP-62 (9.68), HOP-92 (9.14), NCI-H226 (8.49), NCI-H23 (9.47), NCI-H322M (7.48), NCI-H460 (9.51), NCI-H522 (8.62), LXFL-529 (9.44); DMS 114 (9.18), DMS 273 (10.28), COLO 205 (8.77), DLD-1 (8.07), HCC-2998 (7.22), HCT-116 (9.28), HCT-15 (8.47), HT 29 (8.70), KM12 (8.49), KM20L2 (8.70), SW-620 (9.52), SF-268 (8.66), SF-295 (10.36), SF-539 (10.09), SNB-19 (8.77), SNB-75 (10.09), SNB-78 (9.10), U251 (10.19), XF498 (9.23), LOX IMVI (9.62), MALME-3M (8.28), M14 (9.31), M19-MEL (7.32), SK-MEL-2 (9.13), SK-MEL-28 (9.02), SK-MEL-5 (8.46), UACC-257 (8.43), UACC-62 (9.41), IGROV1 (8.66), OVCAR-3 (7.51), OVCAR-4 (7.85), OVCAR-5 (8.00), OVCAR-8 (7.62), SK-OV-3 (8.15), 786-0 (10.11), A498 (9.27), ACHN (8.48), CAKI-1 (9.14), RXF-393 (10.6), SN12C (7.66), TK-10 (7.03), UO-31 (8.38).

ACKNOWLEDGMENTS

The necessary financial support for this investigation was provided by Outstanding Investigator Grant CA 44344-01A1-04-05 and PHS Grant CA-16049-09-12 awarded by the Division of Cancer Treatment, National Cancer Institute, DHHS; the Arizona Disease Control Research Commission; Eleanor W. Libby; the Eagles Art Ehrmann Cancer Fund; Polly Trautman; Lotte Flugel and the Robert B. Dalton Endowment Fund; and for other assistance we thank Drs. Fiona Hogan-Pierson, Yoshitatsu Ichihara, and Ronald A. Nieman; Mr. Lee Williams, Mrs. Kim M. Weiss, the U.S. National Science Foundation (Grants CHE-8409644 and BBS-88-04992) and the NSF Regional Instrumentation Facility in Nebraska (Grant CHE-8620177).

LITERATURE CITED

1. R.L. Berkow, L. Schlabach, R. Dodson, W.H. Benjamin Jr., G.R. Pettit, P. Rustage, and A.S. Kraft, *Cancer Res.*, in press.
2. J.R. Carney, W.Y. Yoshida, and P.J. Scheuer, *J. Org. Chem.*, **57**, 6637 (1992).
3. M. Kobayashi, K. Kawazoe, T. Katori, and I. Kitagawa, *Chem. Pharm. Bull.*, **40**, 1773 (1992).
4. A. Espada, C. Jiménez, J. Rodriguez, P. Crews, and R. Riguera, *Tetrahedron*, **48**, 8685 (1992).
5. M.J. Vázquez, E. Quiñoá, R. Riguera, A.S. Martin, and J. Dárias, *Tetrahedron*, **48**, 6739 (1992).
6. B. Das and K.V.N.S. Srinivas, *J. Nat. Prod.*, **55**, 1310 (1992).
7. C. Djerassi and C.J. Silva, *Acc. Chem. Res.*, **21**, 371 (1991).
8. R.B. Kerr, S.L. Kerr, G.R. Pettit, D.L. Herald, T.L. Groy, and C. Djerassi, *J. Org. Chem.*, **56**, 58 (1991).
9. G.R. Pettit, C.L. Herald, and C.R. Smith, "Biosynthetic Products for Cancer Chemotherapy," Elsevier Scientific, Amsterdam, 1989, Vol. 6.

10. G.R. Pettit, G.M. Cragg, and C.L. Herald, "Biosynthetic Products for Cancer Chemotherapy," Elsevier Scientific, Amsterdam, 1985, Vol. 5.
11. P.J. Scheuer, "Marine Natural Products, Chemical and Biological Perspectives V," Academic Press, New York, 1991, pp. 88–127.
12. G.R. Pettit, M. Inoue, Y. Kamano, D.L. Herald, C. Arm, C. Dufresne, N.D. Christie, J.M. Schmidt, D.L. Doubek, and T.S. Krupa, *J. Am. Chem. Soc.*, **110**, 2006 (1988).
13. G.R. Pettit, M. Inoue, Y. Kamano, C. Dufresne, N.D. Christie, L. Niven, and D.L. Herald, *J. Chem. Soc., Chem. Commun.*, 865 (1988).
14. G.R. Pettit, Y. Kamano, C. Dufresne, M. Inoue, N. Christie, J.M. Schmidt, and D.L. Doubek, *Can. J. Chem.*, **67**, 1509 (1989).
15. G.R. Pettit, Y. Kamano, M. Inoue, C. Dufresne, M.R. Boyd, C.L. Herald, J.M. Schmidt, D.L. Doubek, and N.D. Christie, *J. Org. Chem.*, **57**, 429 (1992).
16. G.R. Pettit, Y. Kamano, R. Aoyagi, C.L. Herald, D.L. Doubek, J.M. Schmidt, and J.J. Rudloe, *Tetrahedron*, **41**, 985 (1985).
17. H. Kessler, C. Griesinger, R. Kerssebaum, K. Wagner, and R.R. Ernst, *J. Am. Chem. Soc.*, **109**, 607 (1987).
18. M.R. Boyd, K.D. Paull, and L.R. Rubinstein, in: "Antitumor Drug Discovery and Development." Ed. by F.A. Valeriote, T. Corbett, and L. Baker, Kluwer Academic Press, Amsterdam, 1992, pp. 11–34.
19. M.R. Boyd, in: "Principles and Practices of Oncology Update." Ed. by V.T. DeVita Jr., S. Hellman, and S.A. Rosenberg, Lippincott, Philadelphia, 1989, Vol. 3, No. 10, pp. 1–12.
20. K.D. Paull, R.H. Shoemaker, L. Hodes, A. Monks, D.A. Scudiero, L. Rubinstein, J. Plowman, and M.R. Boyd, *J. Natl. Cancer Inst.*, **81**, 1088 (1989).
21. A. Monks, D.A. Scudiero, P. Skehan, R.H. Shoemaker, K.D. Paull, D. Vistica, C. Hose, J. Langley, P. Cronise, A. Vaigro-Wolff, M. Gray-Goodrich, H. Campbell, and M.R. Boyd, *J. Natl. Cancer Inst.*, **83**, 757 (1991).
22. M.R. Boyd, in: "Current Therapy in Oncology." Ed. by J.E. Neiderhuber, B.C. Decker, Philadelphia, 1992, pp. 11–22.

Received 26 April 1993